Chinese Chemical Letters 36 (2025) 110250

Contents lists available at ScienceDirect

Chinese Chemical Letters

journal homepage: www.elsevier.com/locate/cclet

Potassium-modified carbon nitride photocatalyzed-aminoacylation of *N*–sulfonyl ketimines

Cailing Wu[a], Shaojie Wu[c], Qifei Huang[a], Kai Sun[c], Xianqiang Huang[b], Jianji Wang[a,*], Bing Yu[c,*]

[a] *Collaborative Innovation Center of Henan Province for Green Manufacturing of Fine Chemicals, Key Laboratory of Green Chemical Media and Reactions, Ministry of Education, School of Chemistry and Chemical Engineering, Henan Normal University, Xinxiang 453007, China*
[b] *School of Chemistry & Chemical Engineering, Liaocheng University, Liaocheng 252059, China*
[c] *College of Chemistry, Zhengzhou University, Zhengzhou 450001, China*

ARTICLE INFO

Article history:
Received 5 May 2024
Revised 11 July 2024
Accepted 15 July 2024
Available online 16 July 2024

Keywords:
Photocatalysis
Amides
Oxamic acids
Aminoacylation
K^+-modified carbon nitride

ABSTRACT

The development of innovative and sustainable catalytic strategies for organic synthesis is a pivotal aspect of advancing material science and chemical engineering. This research presents a new catalytic method for the aminoacylation of *N*–sulfonyl ketimines by utilizing a potassium-doped graphite-like carbon nitride (g-C_3N_4) framework. This method not only enhances the catalytic efficiency and broadens the light absorption spectrum of g-C_3N_4 but also significantly reduces the recombination rate of electron-hole pairs, thereby increasing the reaction yield and selectivity. Importantly, our approach facilitates the synthesis of aminoacylated *N*-heterocycles, expanding the applicability of potassium-modified g-C_3N_4 in photocatalytic organic synthesis. A notable accomplishment of this study is the unprecedented generation of carbamoyl radicals *via* heterogeneous photocatalysis, which can be easily recycled after reaction. This advancement highlights the capability of potassium-doped g-C_3N_4 (namely K-CN) as an advanced heterogeneous photocatalyst for the formation of complex organic compounds.

Amide groups are fundamental structural motifs prevalent in a myriad of molecular entities, encompassing proteins, pharmaceuticals, agrochemicals, medically relevant natural products, and a variety of functional materials [1–3]. The synthesis of amide bonds is pivotal in synthetic chemistry, renowned for its broad application [4]. However, conventional amide bond formation methods primarily involve the coupling of amines with carboxylic acid derivatives, necessitating stoichiometric amounts of dehydrative coupling agents [5]. This dependency introduces significant disadvantages, including the economic and environmental impact due to the agents' toxicity, high cost, and the generation of substantial waste by-products, thus highlighting the critical need for the development of more sustainable, eco-friendly approaches to amide synthesis [6]. The ideal strategies would harness catalytic processes to markedly minimize waste, aligning with the principles of environmentally responsible and green chemistry [7].

In the pursuit of greener synthetic methodologies, photoredox catalysis has emerged as a powerful and gentle platform for a wide array of organic transformations [8–11]. The ability to generate highly reactive radical species through photoredox processes has opened avenues to novel reactivities that are often unattainable through traditional chemical methods [11–15]. For instance, the utilization of carbamoyl radical-mediated processes presents an advanced method for producing amides. Notably, the Melchiorre group has demonstrated the use of redox-active 4-carbamoyl-1,4-dihydropyridine derivatives as carbamoyl radical sources in photo-redox nickel-catalyzed carbamidation of aryl bromides with notable efficacy (Scheme 1a) [16]. Nevertheless, the tedious preparation required for these carbamoyl radical precursors reduces the method's practicality and atom efficiency. The Maiti group has proposed a silyl radical-mediated technique for producing carbamoyl radicals from easily accessible carbamoyl chlorides, applying this method in photoredox nickel-catalyzed carbamidation of aryl bromides (Scheme 1b) [17]. Despite its efficiency, this approach's feasibility is limited by the need for expensive stoichiometric tris(trimethylsilyl)silane, essential for carbamoyl radical generation *via* halogen atom transfer from carbamoyl chloride. Oxamic acids, as stable and non-toxic compounds, can be straightforwardly synthesized by coupling amines with commercially available oxalic acid monoesters [18,19]. The Landais [20] and Song [21] groups developed practical and widely applicable methods for the decarboxylative coupling of oxamic acids with

* Corresponding authors.
E-mail addresses: jwang@htu.edu.cn (J. Wang), bingyu@zzu.edu.cn (B. Yu).

https://doi.org/10.1016/j.cclet.2024.110250
1001-8417/

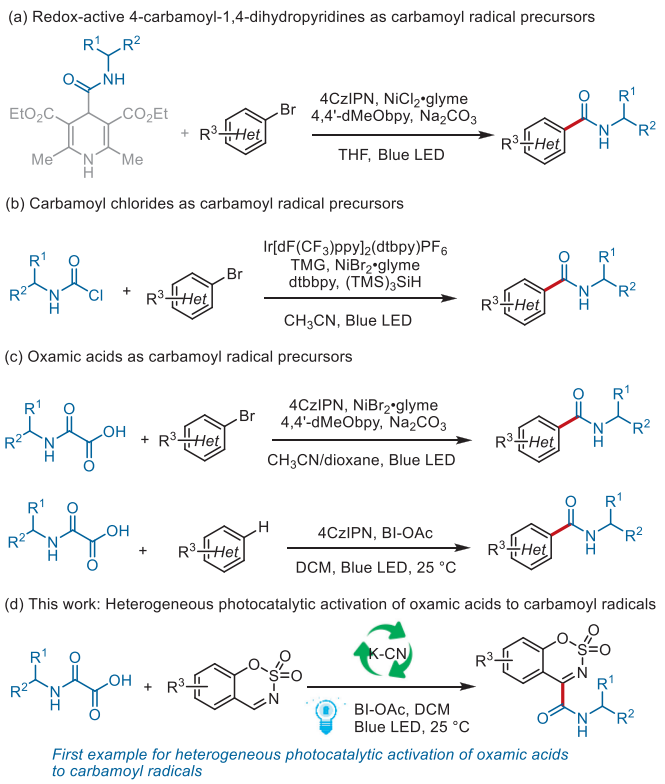

Scheme 1. Carbamoyl radical-mediated amide synthesis.

heteroarenes or (hetero)aryl halides (Scheme 1c). In those previous studies, non-recyclable photocatalysts were used, which limited their practical applications. Therefore, the development of reusable and cost-efficient heterogeneous photocatalysts is attractive for industrial utilization.

Graphite-like carbon nitride (g-C_3N_4), consisting of the readily available elements carbon and nitrogen, has been extensively applied in various areas of photocatalytic chemistry, including the photocatalytic degradation of organic pollutants, CO_2 reduction, and water splitting [22–27]. However, the practical application of g-C_3N_4 faces several challenges, such as limited active sites, inadequate light absorption, and the swift recombination of photoinduced electron-hole pairs. To overcome these obstacles, recent advancements have introduced innovative modification techniques like exfoliation, morphological tuning, doping, and the creation of heterojunctions, all aimed at enhancing the photocatalytic performance of g-C_3N_4 [28–30]. Among these, porous heteroatom-doped g-C_3N_4 nanosheets have emerged as versatile heterogeneous photocatalysts, exhibiting improved light absorption, facilitated charge carrier migration, and an increased count of accessible active sites for catalysis. Additionally, these modifications often result in an optimized electronic structure, significantly enhancing the redox potential which is crucial for photocatalytic reactions such as photocatalytic oxidation of alcohols to aldehydes [31], and photoreduction of CO_2 to CO [32]. Despite these significant advances, the utilization of porous heteroatom-doped g-C_3N_4 in photocatalytic organic transformations, especially the synthase of amides is still in its nascent stages, presenting fertile ground for further research and innovation [26].

With our ongoing interest in the development of green synthetic methods [33–36], herein, we developed potassium-modified carbon nitride (K-CN) from bulk g-C_3N_4 through a process characterized by low-temperature and short-duration calcination. Compared to its precursor, K-CN demonstrates markedly improved efficiency in the separation of photogenerated charge carriers, heightened light responsiveness, and superior light absorption capacity. Significantly, the use of K-CN as a heterogeneous photocatalyst enabled the carbamylation of nitrogen-containing heterocycles under visible light (Scheme 1d). To the best of our knowledge, this is the first example of the generation of carbamoyl radicals under heterogeneous photocatalysis. This research paves the way for the development of innovative heterogeneous photocatalysts and expands their utility in organic synthesis, marking a notable advancement in photocatalytic science.

The synthesis of potassium-modified graphitic carbon nitride (K-CN) was carried out by slightly modifying a previously established method [37], as detailed schematically in Fig. S1 (Supporting information). The initial step involved the synthesis of graphitic carbon nitride (g-C_3N_4) through the thermal decomposition of melamine. This process required heating the melamine to 550 °C for 5 h in a ceramic crucible, under a nitrogen atmosphere. Subsequently, a potassium-enriched variant of g-C_3N_4 (K-CN) was fabricated using a molten-salt technique, employing a KCl/LiCl eutectic mixture as the reaction medium.

The detailed synthesis procedure is as follows: A mixture of 0.5 g of g-C_3N_4 and 2 g of KCl/LiCl (with a molar ratio of 0.56:1) was thoroughly ground in a mortar for 5 min. The homogenized mixture was then transferred to a porcelain boat and heated in a tubular furnace filled with nitrogen gas. The temperature was increased at a controlled rate of 5 °C/min up to 550 °C and maintained at this level for 1.5 h. Upon cooling to ambient temperature, the resultant solid was dispersed in deionized water (maintained at 80 °C for 3 h), followed by filtration. The filtered yellow solid powder was subsequently dried in a vacuum oven at 60 °C for 12 h to yield the catalyst K-CN-2. Variants of this catalyst denoted as K-CN-X (X = 4, 6, where X signifies the mass in grams of KCl/LiCl added per 0.5 g of g-C_3N_4), were synthesized analogously, demonstrating the adaptability of the procedure to produce a series of potassium-modified catalysts. In the preparation of K-CN samples, the inclusion of LiCl plays a crucial role in reducing the calcination temperature needed for catalyst formation, enabling the preparation of the catalyst at temperatures below 550 °C.

N-Sulfonyl ketimines, bearing essential sulfur and nitrogen moieties, are quintessential heterocyclic components pervasive in a myriad of pharmaceuticals and bioactive compounds [38,39]. The strategic functionalization of *N*-sulfonyl ketimines is recognized as a pivotal methodology to enhance their physicochemical properties, thus elevating their therapeutic potential and paving new paths in the realm of drug discovery [40,41]. In pursuit of these scientific endeavors, our study embarked on an exploratory synthetic approach, engaging in a reaction between 6-chlorobenzo[*e*][1,2,3]oxathiazine 2,2-dioxide (**1a**) and 2-(cyclohexylamino)−2-oxoacetic acid (**2a**), as depicted in Table 1.

It is particularly encouraging that, under conditions utilizing K-CN-2 (20 mg) as a photocatalyst, dichloromethane (DCM, 1 mL) as the solvent, and 1-acetoxy-1,2-benzo[*d*]iodoxol-3(1*H*)-one (BI-OAc, 0.15 mmol) as the oxidant, with 460 nm blue light irradiation for 5 h, we were able to isolate the target product **3a** with a yield of 72% (entry 1). In our endeavor to enhance the efficiency of chemical reactions, we explored in depth the impact of various solvents on the reactions. This exploration included a wide array of solvents (entries 2–9), such as ethanol (EtOH), acetonitrile (MeCN), 1,2-dichloroethane (DCE), dimethyl carbonate (DMC), *N*,*N*-dimethylformamide (DMF), dimethyl sulfoxide (DMSO), ethyl acetate (EA), and water (H_2O). Our findings revealed that employing DCE or DMSO as solvents facilitated the synthesis of the target product **3a** with yields of 34% and 42%, respectively (entries 2 and 3). The inability of other solvents to yield the desired product highlighted the critical importance of solvent selection in the reaction process (entries 4–9). Subsequently, we examined the in-

Table 1
Optimization of reaction conditions.[a]

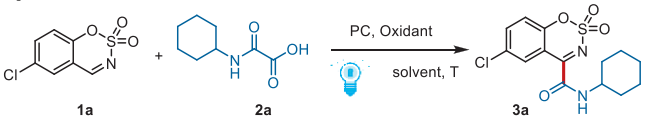

Entry	Photocatalyst	Oxidant	Solvent	Yield (%)
1	K-CN-2	BI-OAc	DCM	72
2	K-CN-2	BI-OAc	DCE	42
3	K-CN-2	BI-OAc	DMSO	34
4	K-CN-2	BI-OAc	CH_3CN	Trace
5	K-CN-2	BI-OAc	DMC	Trace
6	K-CN-2	BI-OAc	DMF	Trace
7	K-CN-2	BI-OAc	EtOH	Trace
8	K-CN-2	BI-OAc	EA	Trace
9	K-CN-2	BI-OAc	H_2O	Trace
10	K-CN-2	$PhI(OAc)_2$	DCM	65
11	K-CN-2	$PhI(TFA)_2$	DCM	25
12	K-CN-2	BI-OH	DCM	35
13	K-CN-4	BI-OAc	DCM	78
14	K-CN-6	BI-OAc	DCM	83
15[b]	K-CN-6	BI-OAc	DCM	72
16	–	BI-OAc	DCM	N.D.
17[c]	g-C_3N_4	BI-OAc	DCM	16
18	g-C_3N_4	BI-OAc	DCM	13
19	K-CN-6	–	DCM	17
20[d]	K-CN-6	BI-OAc	DCM	N.D.

[a] Reaction conditions: **1a** (0.1 mmol), **2a** (0.2 mmol), oxidant (0.15 mmol), solvent (2 mL), PC (20 mg), 460 nm blue LED (10 W), 5 h, under air. Isolated yields were given based on **1a**. N.D. = not detected. BI-OH = hydroxybenziodoxole.
[b] 15 mg K-CN-6.
[c] 2 equiv. of KCl and LiCl were added.
[d] In darkness.

fluence of various oxidants on the reaction (entries 10–12), where BI-OAc emerged as the superior option. Further analysis of catalysts showed that all the synthesized catalysts were effective in promoting the reaction (entries 13 and 14). Interestingly, an increase in the use of KCl/LiCl enhanced the catalytic efficiency of the calcined catalysts, with K-CN-6 proving to be the most effective photocatalyst (entry 14). Nevertheless, diminishing the amount of catalyst gradually reduced the reaction yield (entry 15), and in the absence of a photocatalyst, the reaction cannot proceed (entry 16). The use of g-C_3N_4 as a catalyst delivered the desired product **3a** with only 16% yield, signifying the need for its modification (entry 17). The introduction of 2 equiv. of KCl and 2 equiv. of LiCl into the reaction system, alongside g-C_3N_4 as the photocatalyst, failed to markedly improve the reaction with only 13% yield of the desired product, indicating the essentiality of catalyst calcination for enhanced efficacy (entry 18). Moreover, the control experiments showed that the reaction was significantly impeded in the absence of oxidants or light, highlighting their indispensable roles in the reaction facilitation process (entries 19 and 20). Consequently, the optimal reaction conditions were established to be: **1a** (0.1 mmol), **2a** (0.2 mmol), with K-CN-6 (20 mg) serving as the photocatalyst, 1.5 equiv. of bis(imidazole-1-yl)acetate (BI-OAc) as the oxidant, and dichloromethane (DCM) as the solvent, all under blue light irradiation (entry 14).

In order to understand the excellent catalytic performance of K-CN, we carried out some characterizations of the materials. The formation of bulk g-C_3N_4 and K-CN samples was confirmed by scanning electron microscope (SEM), X-ray photoelectron spectroscopy (XPS), and X-ray diffraction (XRD) patterns. As shown in Figs. 1a and b, the K-CN-6 particles are smaller and more uniform than the g-C_3N_4 particles. g-C_3N_4 has an aggregated and stacked structure, while K-CN-6 has an aggregated granular structure. The chemical composition and chemical state of corresponding elements on the surface of K-CN-6 and g-C_3N_4 were investigated by X-ray photoelectron spectroscopy (XPS), and the XPS spectra for N element are shown in Figs. 1d and e. The survey XPS spectra show that g-C_3N_4 is composed of C, N, and O elements, while K-CN-6 is composed of C, N, O, and K elements, and no Li and Cl elements are found, suggesting that K rather than the form of KCl exists in K-CN-6. The N 1s spectra of K-CN-6 in Fig. 1e exhibit three peaks at 398.7 eV, 399.7 eV, and 401.4 eV, ascribing to the sp^2 hybrid nitrogen atom (C–N=C), the sp^3 hybrid N-amino band connected to the structural motif on the carbon nitride skeleton (N–C_3) and the N–H bond of the amino group, respectively. The area ratios of N–H/C–N=C decrease from 0.35 (g-C_3N_4) to 0.20 (K-CN-6), indicating the amido groups of K-CN-6 are modified by K, this result proves that K was successfully introduced.

In the XRD patterns (Fig. 1c), g-C_3N_4 shows two obvious diffraction peaks at $2\theta = 12.9°$ and 27.7° values assigned to (100) and (002) crystal facets, respectively. While the peak of (100) crystal facet was weakened in K-CN samples, new peaks at 8.0° related to (110) crystal facet appeared, indicating that crystalline structure is changed to a certain extent. It should be noted that the peak value of (002) crystal facet of K-CN samples slightly increased along with the mass increase KCl/LiCl, indicating that the interlayer spacing becomes smaller because of the K doping content increased. It has been demonstrated that K could bridge the adjacent layers of g-C_3N_4 to build an electron delivery channel, which would accelerate directional electron transfer between layers and suppress random charge transfer between the planes of g-C_3N_4 [42].

Photoluminescence (PL) emission and the transient photocurrent (TPC) were conducted to confirm the acceleration of K on directional electron transfer. As shown in Fig. 1g, K-CN-6 exhibits a weaker PL intensity compared with g-C_3N_4, suggesting that the separation ability of photo-generated charge carriers in the K-CN-6 photocatalyst is higher than that in g-C_3N_4. Furthermore, the TPC response confirmed the high photocatalytic activity of K-CN-6 (Fig. 1h), as the photogenerated carriers can be effectively separated. These results showed that the photoelectrochemical properties of g-C_3N_4 were significantly improved by introducing K. Fourier transform infrared spectroscopy (FT-IR) was commonly used to investigate the functional group characteristics of catalysts. As observed from the FT-IR spectra of Fig. 1f, similar peaks at 1200 cm^{-1} to 1650 cm^{-1} and 809 cm^{-1} exist in g-C_3N_4 and K-CN-6, attributing to heterocyclic ring and triazine structure, respectively. It should be noted that the intensity of the broadband at 3000 cm^{-1} to 3300 cm^{-1}, corresponding to the stretching modes of N–H in terminal amino groups, in K-CN-6 is significantly reduced compared to g-C_3N_4. It proves that K takes the place of H atoms in amino groups and is connected with N atoms [43]. The interaction between K and N would influence the band edge of the conduction band (CB) minimum and the valence band (VB) maximum, and further influence the band gap (E_g), because of the different abilities of donating electrons by K and H atoms to g-C_3N_4 [44]. Then the energy-gap structures of K-CN-6 and g-C_3N_4 are investigated by UV–vis absorption spectra. As shown in Fig. 1i, the absorption edges of K-CN-6 show an obvious expansion from 460 nm (g-C_3N_4) to 480 nm (K-CN-6) at the visible light region, as the band gap decreases from 2.73 eV (g-C_3N_4) to 2.58 eV (K-CN-6). This result demonstrates the effect of K introduction on visible light absorption.

Upon optimizing the reaction conditions, the scope of the transformation involving various substituted benzo[*e*][1,2,3]oxathiazine 2,2-dioxides **1** with 2-(cyclohexylamine)–2-oxo-acetic acid **2a** was explored under visible light irradiation. It turns out that substrate **1** bearing with a wide array of substituents ranging from electron-donating to electron-withdrawing groups such as -F, -Cl, -Br, -I, -CO_2Me, and -OMe on the benzene ring, were integrated into the reaction. This versatility in functional group compatibility facilitated the synthesis of the corresponding prod-

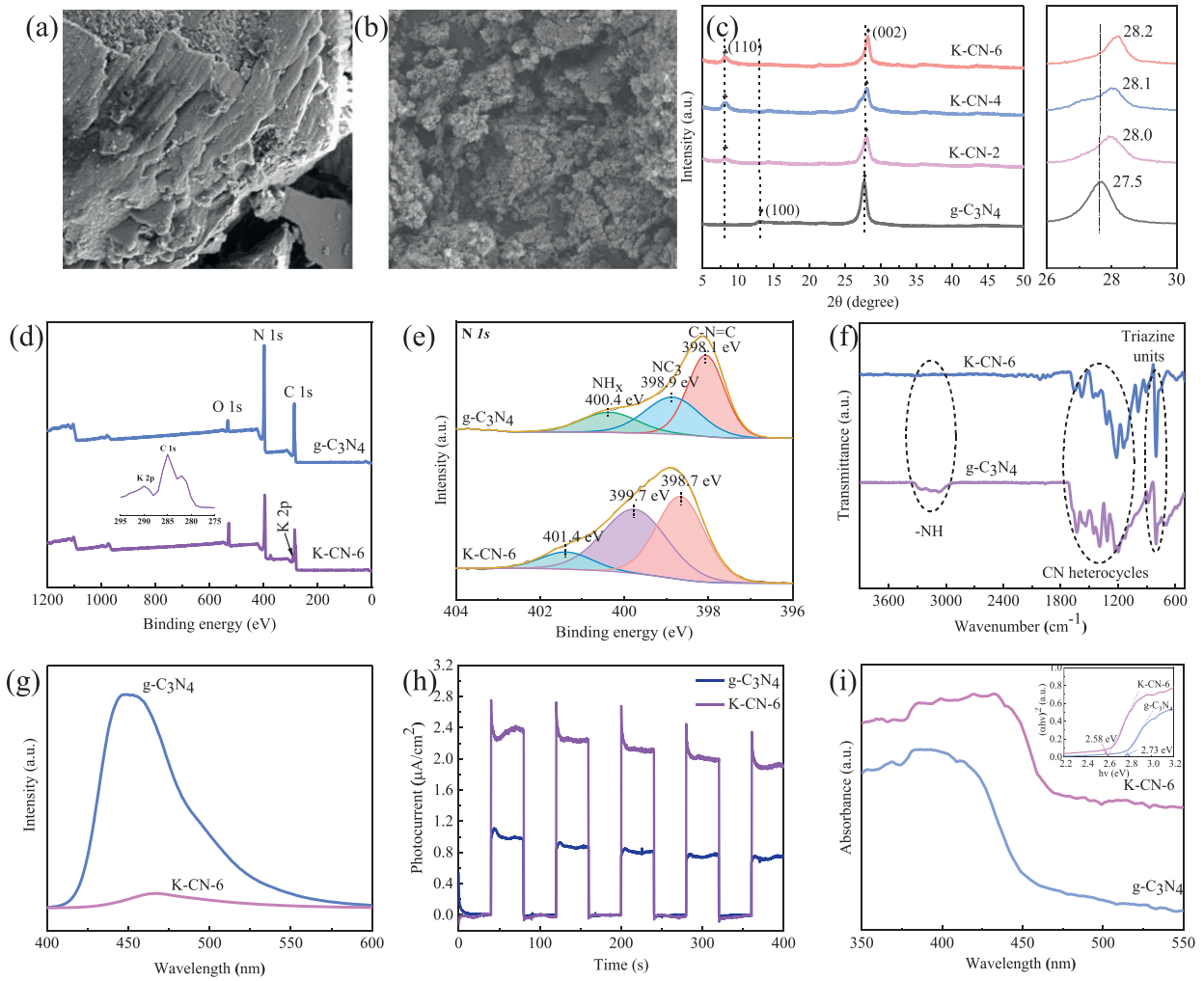

Fig. 1. Characterizations and photoelectric properties of K-CN-6 and g-C_3N_4. (a) SEM image of g-C_3N_4. (b) SEM image of K-CN-6. (c) XRD patterns. (d) Survey XPS spectra. (e) High-resolution N 1s spectrum. (f) FT-IR spectra. (g) PL spectra. (h) Transient photocurrent. (i) UV/vis DRS spectra and the plots of $(\alpha h\nu)^2$ *vs.* photon energy (hν) (insert).

ucts (**3a**-**3j**) in moderate to high yields. Notably, unsubstituted benzo[*e*][1,2,3]oxathiazine 2,2-dioxide facilitated the synthesis of the desired product **3f** with a 67% yield. Exceptionally, the substrate featuring an allyl substituent exhibited superior reactivity and selectivity, yielding the targeted product (**3j**) with a 72% yield. This result suggests that the process was not hindered by the presence of a terminal alkene group, as evidenced by the absence of by-products involving the double bond. Moreover, benzo[*e*][1,2,3]oxathiazine 2,2-dioxides bearing two different functional groups also successfully furnished the targeted products (**3k**, **3l**, and **3m**) with yields of 73%, 76%, and 75%, respectively. In contrast, the derivative substituted with di–*tert*–butyl groups demonstrated a marked reduction in reactivity, culminating in a diminished yield of 42% for product **3n**, presumably due to steric hindrance from the bulky substituents.

Subsequently, the reactivity profile of *N*-substituted oxamic acids **2** was further delineated through reactions with 6-chlorobenzo[*e*][1,2,3]oxathiazine 2,2-dioxides **1a**. These substituents such as cyclopentane and neopentane on the nitrogen atom significantly contributed to the synthesis of the corresponding products **3o** and **3p** in commendable yields. The introduction of a phenylethyl substituent on the nitrogen atom led to the synthesis of the target product **3q** with a 68% yield. Conversely, employing amantadine-substituted oxamic acid failed to yield the anticipated product, delineating a specific limitation in the substrate scope under the conditions investigated. Moreover, when 2-oxo-2-(phenylamino)acetic acid or 2-(dimethylamino)–2-oxoacetic acid were employed as subtracts, the desired products **3s** and **3t** could not be detected. This implies that 2-oxo-2-(phenylamino)acetic acid and 2-(dimethylamino)–2-oxoacetic acid are not suitable substrates for this transformation (Scheme 2).

Afterward, the reusability of the photocatalyst K-CN-6 was evaluated. This catalyst was conveniently separated from the reaction mixture *via* centrifugation. Analysis of the XRD patterns for the recovered K-CN-6 after repeated use revealed notable changes: the intensity of the diffraction peak at the (110) plane at 8.2° diminished, and the peak corresponding to the (002) plane shifted from 28.1° to 27.6°. These observations suggest a progressive loss of K atoms from the catalyst K-CN-6, as illustrated in Fig. S3 (Supporting information). Furthermore, by the third cycle of recovery, there was a marked reduction in the yield of the desired product, attributed to the continuous depletion of K^+ ions (for details see Supporting information).

To advance our understanding of the reaction mechanisms, a series of rigorously planned control experiments were undertaken under optimal conditions. The addition of 10 equiv. of the radical inhibitor 2,2,6,6-tetramethyl-1-piperidinyloxy (TEMPO) to the prototype reaction markedly attenuated its reactivity (Table 2, entry 1). The decrease in activity suggests a radical-mediated mechanism, a proposition further supported by the detection of a radical adduct through high-resolution mass spectrometry, indicative of the generation of a carbamoyl radical (for details see

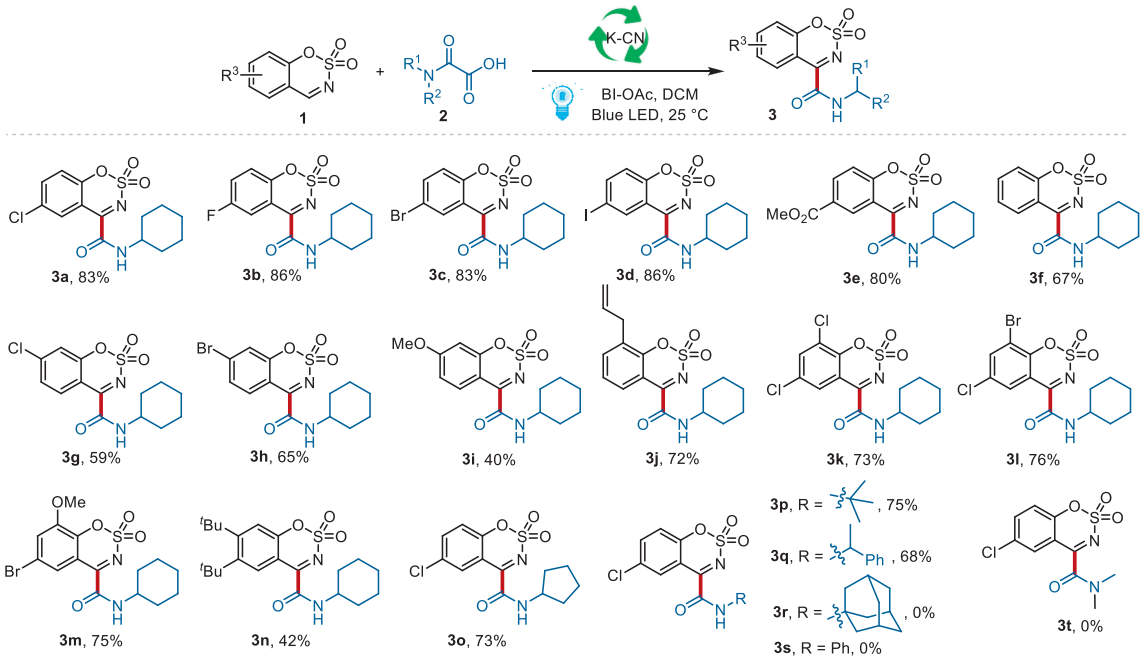

Scheme 2. Substrate scope. Reaction conditions: **1** (0.1 mmol), **2** (0.2 mmol), BI-OAc (1.5 equiv.), K-CN-6 (20 mg), DCM (1 mL), 10 W blue LED (460 nm), 5 h, under air. Isolated yields were given based on **1**.

Table 2
Control experiments.[a]

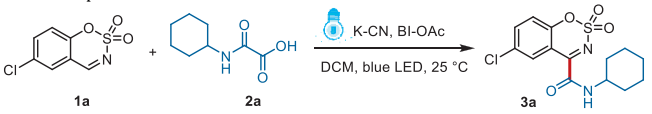

Entry	Deviation from standard conditions	Yield
1	TEMPO (10 equiv.) was added	Trace
2	AO (10 equiv.) was added	Trace
3	$K_2S_2O_8$ (10 equiv.) was added	Trace
4	N_2 instead of air	Trace
5	BQ (10 equiv.) was added	Trace

[a] Reaction conditions: **1a** (0.1 mmol), **2a** (0.2 mmol), BI-OAc (1.5 equiv.), DCM (2 mL), K-CN-6 (20 mg), 10 W blue LED (460 nm), 5 h, under air.

Supporting information). Furthermore, the integration of 10 equiv. of ammonium oxalate (AO), a known hole scavenger, nearly halted the reaction (Table 2, entry 2), while the introduction of 10 equiv. of potassium persulfate ($K_2S_2O_8$), an electron scavenger, significantly diminished the yield (Table 2, entry 3). These outcomes highlight the critical roles of photo-generated electrons and holes in the reaction's mechanistic pathway. Performing the reaction in a nitrogen environment substantially hindered its progression, thus confirming the crucial involvement of oxygen in the reaction's mechanism (Table 2, entry 4). Additionally, incorporating 10 equiv. of benzoquinone (BQ), a scavenger of superoxide radical anion, led to the production of only trace amounts of the target product, underscoring the crucial involvement of superoxide radical anion in facilitating the reaction (Table 2, entry 5).

Considering experimental insights and previous reports, we proposed a mechanism outlined in Scheme 3. Initially, K-CN creates the photogenerated separation of electron-hole pairs under visible

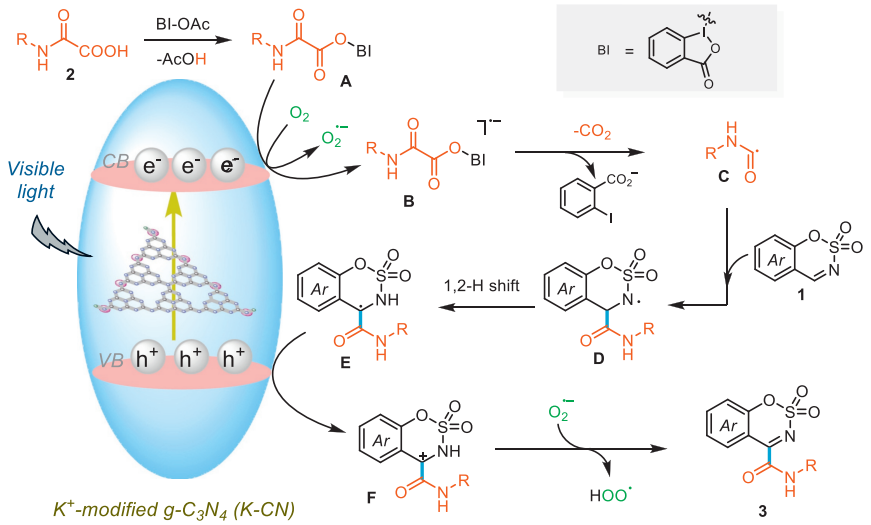

Scheme 3. Proposed mechanism.

light illumination. These charge carriers may subsequently drive redox reactions when they migrate to the surface. Meanwhile, the reaction between oxamic acids **2** and BI-OAc leads to the formation of intermediate **A**. Afterward, intermediate **A** is reduced within the conduction band (CB) to produce the radical anion **B**. Following this, radical anion **B** undergoes decarboxylation to yield the carbamoyl radical **C**. Concurrently, molecular oxygen (O_2) undergoes reduction at the CB, resulting in the production of the superoxide radical anion ($O_2^{\bullet-}$). The carbamoyl radical **C** subsequently interacts with the C=N double bond of substrate **1**, resulting in the formation of the nitrogen-centered radical **D**. Radical **D** then experiences a 1,2-hydrogen shift, leading to the creation of radical **E**. Subsequently, radical **E** engages in a single electron transfer event, resulting in the generation of intermediate **F**. Ultimately, intermediate **F** undergoes a hydrogen atom transfer (HAT) process with the superoxide radical anion, culminating in the production of the desired product **3**.

In conclusion, we have developed a novel and efficient catalytic strategy for the aminoacylation of *N*–sulfonyl ketimines, utilizing a potassium-doped g-C_3N_4 framework. This method significantly amplifies the catalytic efficiency and light absorption capabilities of g-C_3N_4, while substantially diminishing the recombination rate of electron-hole pairs. Moreover, it offers an innovative approach for the synthesis of aminoacylated nitrogen heterocycles, thereby broadening the scope of potassium-modified g-C_3N_4 in organic chemical synthesis. Remarkably, to the best of our knowledge, this study marks the first instance of carbamoyl radicals being generated through heterogeneous photocatalysis, which can be easily recycled after reaction. This achievement opens new avenues in the development of sophisticated heterogeneous photocatalysts and extends their utility in the crafting of organic compounds, representing a significant advancement in photocatalytic science. We anticipate that the photoinduced activation strategy mediated by potassium-modified carbon nitride for aminoacylation will become increasingly prevalent in organic synthetic methodologies, providing a greener and more efficient method for the assembly of diverse and complex molecular architectures.

Declaration of competing interests

The authors declare that they have no known competing financial interests or personal relationships that could have appeared to influence the work reported in this paper.

The author is an Editorial Board Member for Chinese Chemical Letters and was not involved in the editorial review or the decision to publish this article.

CRediT authorship contribution statement

Cailing Wu: Writing – review & editing, Writing – original draft, Methodology, Investigation, Conceptualization. **Shaojie Wu:** Writing – original draft, Methodology, Investigation. **Qifei Huang:** Writing – original draft, Methodology. **Kai Sun:** Writing – review & editing, Writing – original draft, Methodology, Investigation, Conceptualization. **Xianqiang Huang:** Writing – original draft, Methodology. **Jianji Wang:** Writing – review & editing, Supervision, Conceptualization. **Bing Yu:** Writing – review & editing, Writing – original draft, Supervision, Project administration, Methodology, Investigation, Funding acquisition, Conceptualization.

Acknowledgments

We acknowledge the financial support from the National Natural Science Foundation of China (No. 22171249), and the Science & Technology Innovation Talents in Universities of Henan Province (No. 23HASTIT003).

Supplementary materials

Supplementary material associated with this article can be found, in the online version, at doi:10.1016/j.cclet.2024.110250.

References

[1] V.R. Pattabiraman, J.W. Bode, Nature 480 (2011) 471–479.
[2] S.D. Roughley, A.M. Jordan, J. Med. Chem. 54 (2011) 3451–3479.
[3] D.G. Brown, J. Boström, J. Med. Chem. 59 (2016) 4443–4458.
[4] E. Valeur, M. Bradley, Chem. Soc. Rev. 38 (2009) 606–631.
[5] P. Acosta-Guzmán, A. Ojeda-Porras, D. Gamba-Sánchez, Adv. Synth. Catal. 365 (2023) 4359–4391.
[6] H.C. Li, G.N. Li, K. Sun, et al., Org. Lett. 24 (2022) 2431–2435.
[7] M.T. Sabatini, L.T. Boulton, H.F. Sneddon, T.D. Sheppard, Nat. Catal. 2 (2019) 10–17.
[8] F. Gao, S. Zhang, Q. Lv, B. Yu, Chin. Chem. Lett. 33 (2022) 2354–2362.
[9] Z. Chen, J. Chen, J. Xuan, Chin. Chem. Lett. 33 (2022) 2763–2764.
[10] W. Cui, Y. Li, X. Li, et al., Chin. Chem. Lett. 34 (2023) 107477.
[11] W.T. Ouyang, H.T. Ji, J. Jiang, et al., Chem. Commun. 59 (2023) 14029–14032.
[12] M. Ding, S. Zhou, S. Yao, et al., Chin. J. Chem. 42 (2024) 351–355.
[13] C.L. Ji, X. Zhai, Q.Y. Fang, et al., Chem. Soc. Rev. 52 (2023) 6120–6138.
[14] Y. Lv, H. Ding, J. You, W. Wei, D. Yi, Chin. Chem. Lett. 35 (2024) 109107.
[15] Z. Wang, N. Meng, Y. Lv, et al., Chin. Chem. Lett. 34 (2023) 107599.
[16] N. Alandini, L. Buzzetti, G. Favi, et al., Angew. Chem. Int. Ed. 59 (2020) 5248–5253.
[17] S. Maiti, S. Roy, P. Ghosh, A. Kasera, D. Maiti, Angew. Chem. Int. Ed. 61 (2022) e202207472.
[18] I.M. Ogbu, G. Kurtay, F. Robert, Y. Landais, Chem. Commun. 58 (2022) 7593–7607.
[19] C. Ma, Y. Tian, J. Wang, et al., Org. Lett. 24 (2022) 8265–8270.
[20] A.H. Jatoi, G.G. Pawar, F. Robert, Y. Landais, Chem. Commun. 55 (2019) 466–469.
[21] D. Duan, L. Song, Org. Chem. Front. 11 (2024) 47–52.
[22] Y. Xing, X. Wang, S. Hao, et al., Chin. Chem. Lett. 32 (2021) 13–20.
[23] Q. Hu, Y. Dong, K. Ma, X. Meng, Y. Ding, J. Catal. 413 (2022) 321–330.
[24] B. Dam, A.K. Sahoo, B.K. Patel, Green Chem. 24 (2022) 7122–7130.
[25] Y. Guo, R. Chang, Z. Fu, C.Y. Zhou, Z. Guo, Green Chem. 25 (2023) 5206–5212.
[26] S.K. Verma, R. Verma, Y.R. Girish, et al., Green Chem. 24 (2022) 438–479.
[27] F.L. Zeng, H.L. Zhu, X.L. Chen, L.B. Qu, B. Yu, Green Chem. 23 (2021) 3677–3682.
[28] T. Shi, Y.T. Liu, S.S. Wang, Q.Y. Lv, B. Yu, Chin. J. Chem. 40 (2022) 97–103.
[29] Z. Chen, B. Chong, N. Wells, G. Yang, L. Wang, Chin. Chem. Lett. 33 (2022) 2579–2584.
[30] C. Wang, B. Wei, H. Zhu, et al., Chin. Chem. Lett. 33 (2022) 3073–3077.
[31] G. Marcì, E.I. García-López, F.R. Pomilla, et al., Catal. Today 328 (2019) 21–28.
[32] S. Hu, P. Qiao, Z. Liu, et al., J. Catal. 432 (2024) 115405.
[33] A. Shi, K. Sun, Y. Wu, et al., J. Catal. 415 (2022) 28–36.
[34] S.J. Wu, Y. Shi, K. Sun, et al., J. Catal. 415 (2022) 87–94.
[35] C. Ge, L. Qiao, Y. Zhang, et al., Chin. J. Chem. 42 (2024) 1679–1685.
[36] Z. Zhang, F. Cheng, X. Ma, et al., Green Chem. 26 (2024) 7331–7336.
[37] H. Jing, L. Chen, S. Yi, et al., Chem. Eng. J. 417 (2021) 129187.
[38] H.Y. Song, J. Jiang, Y.H. Song, et al., Chin. Chem. Lett. 35 (2024) 109246.
[39] Y.H. Lu, C. Wu, J.C. Hou, et al., ACS Catal. 13 (2023) 13071–13076.
[40] Y.H. Lu, S.Y. Mu, H.X. Li, et al., Green Chem. 25 (2023) 5539–5542.
[41] H.Y. Song, F. Xiao, J. Jiang, et al., Chin. Chem. Lett. 34 (2023) 108509.
[42] J. Li, W. Cui, Y. Sun, et al., J. Mater. Chem. A 5 (2017) 9358–9364.
[43] X. Sun, D. Jiang, L. Zhang, W. Wang, Appl. Catal. B: Environ. 220 (2018) 553–560.
[44] T. Xiong, W. Cen, Y. Zhang, F. Dong, ACS Catal. 6 (2016) 2462–2472.